WR0108 UK SUPPORT FOR EU LEACHXS EXPERT DATABASE ON WASTE CHARACTERISATION

ANNEX D3 - Mechanistic modeling of GSF lysimeter data with LeachXS-Orchestra

H.A. van der Sloot

The GSF lysimeter data have been kindly supplied by SIWAP (the German Sickerwasserprognose Project). Data had previously been obtained from BAM on the laboratory test results for the pH dependence test. These results have been modeled to provide a basis for the modeling of the lysimeter data. pH dependence test data for the soil used in the GSF lysimeter are missing. So to be able to model the transport to soil and groundwater we have applied data for a rather weak sandy soil.

ECN, Vanderbilt and DHI jointly developed a modeling approach in the framework of the LeachXS database/expert system development. This uses a Chemical Speciation Fingerprint for all subsequent calculations with a given material using Orchestra as the geochemical speciation code. A 3-layer model was set up to describe release from MSWI bottom ash into the soil in a lysimeter configuration (GSF).

First the pH dependence test data were modeled using LeachXS-Orchestra to provide a Chemical Speciation Fingerprint (CSF). The full mechanistic modeling requires as input "availability" data (derived from the maximum concentration as measured in the pH stat), a quantification of reactive surfaces Fe-oxide, Al-oxide, clay and dissolved and particulate organic matter (the latter data have been taken from other sources, as these data are not available for the bottom ash nor for the soil). In Table I the parameters used are given.

Table I. Parameters for prediction of pH dependence test data

Input specification

Speciation session	MSWI BAM
Material	BAM_RMMV (P,1,1)

Solved fraction DOC			**DOC/DHA**	**pH**	**[DOC] (kg/l)**	**DHA fraction**	**[DHA] (kg/l)**	**Polynomial coeficients**	
Sum of pH and pe	15.00			1.00	3.000E-05	0.20	6.000E-06	**C0**	-5.004E+00
L/S	10.0000			4.00	1.200E-05	0.20	2.400E-06	**C1**	-2.202E-01
Clay	1.000E-02	**kg/kg**		7.00	8.000E-06	0.20	1.600E-06	**C2**	1.518E-02
HFO	2.000E-04	**kg/kg**		11.00	8.000E-06	0.30	2.400E-06	**C3**	0.000E+00
SHA	2.000E-04	**kg/kg**		14.00	2.000E-05	0.40	8.000E-06	**C4**	0.000E+00
								C5	0.000E+00

Reactant concentrations

Reactant	**mg/kg**	**Reactant**	**mg/kg**	**Reactant**	**mg/kg**	**Reactant**	**mg/kg**	**Reactant**	**mg/kg**
Ag+	not measured	Cd+2	1.029E+00	Hg+2	not measured	Na+	1.525E+03	Sb[OH]6-	not measured
Al+3	2.222E+03	Cl-	3.500E+03	I-	not measured	NH4+	not measured	SeO4-2	not measured
H3AsO4	1.051E-01	CrO4-2	7.333E-01	K+	8.289E+02	Ni+2	3.726E+00	H4SiO4	8.848E+02
H3BO3	not measured	Cu+2	6.038E+01	Li+	not measured	NO3-	not measured	Sr+2	4.148E+01
Ba+2	1.974E+00	F-	5.000E+01	Mg+2	7.645E+02	PO4-3	5.000E+02	UO2+	not measured
Br-	not measured	Fe+3	1.126E+02	Mn+2	6.604E+01	Pb+2	1.676E+01	VO2+	2.056E-01
Ca+2	2.402E+04	H2CO3	2.100E+04	MoO4-2	6.697E-01	SO4-2	2.446E+03	Zn+2	5.252E+02

Selected Minerals

AA_2CaO_Al2O3_8H2O[s]	AA_Portlandite	Cu[OH]2[s]
AA_2CaO_Al2O3_SiO2_8H2O[s]	AA_Tobermorite-I	Fe_Vanadate
AA_2CaO_Fe2O3_8H2O[s]	AA_Tobermorite-II	Fluorite
AA_3CaO_Al2O3[Ca[OH]2]0_5_[CaCO3]0_5_11_	AA_Tricarboaluminate	Magnesite
AA_3CaO_Al2O3_CaCO3_11H2O[s]	Albite[low]	Ni[OH]2[s]
AA_3CaO_Fe2O3_6H2O[s]	Antlerite	Pb[OH]2[C]
AA_4CaO_Al2O3_13H2O[s]	Ba[SCr]O4[77%SO4]	Pb2V2O7
AA_Al[OH]3[am]	BaSrSO4[50%Ba]	Pb3[VO4]2
AA_Brucite	Birnessite	PbCrO4
AA_Calcite	Brochantite	PbMoO4[c]
AA_CaO_Al2O3_10H2O[s]	Bunsenite	P-Wollstanite
AA_Fe[OH]3[microcr]	Ca2Cd3[PO4]3Cl	Pyrolusite
AA_Gibbsite	Ca3Cd2[PO4]3Cl	Rhodochrosite
AA_Gypsum	Cd[OH]2[A]	Strontianite
AA_Jennite	Cd4[OH]6SO4	Wairakite
AA_Magnesite	Cr[OH]3[C]	Willemite

Availabilities for Si, P, carbonate, Fe and V, as well as clay, Fe-oxide and solid organic matter were missing from the BAM dataset and taken from Dutch information on bottom ash. The number of pH conditions analysed were rather limited for this kind of modeling. A minimum number of 8 steps is recommended in the European standard TS 14429. When the missing parameters can be generated on the materials studied, a much better prediction of behaviour will be possible as presented in Dijkstra *et al.* (2008)[1].

In Appendix A results of the model prediction and the partitioning between dissolved and particulate phases is provided. In Figure 1 an example of the data is given.

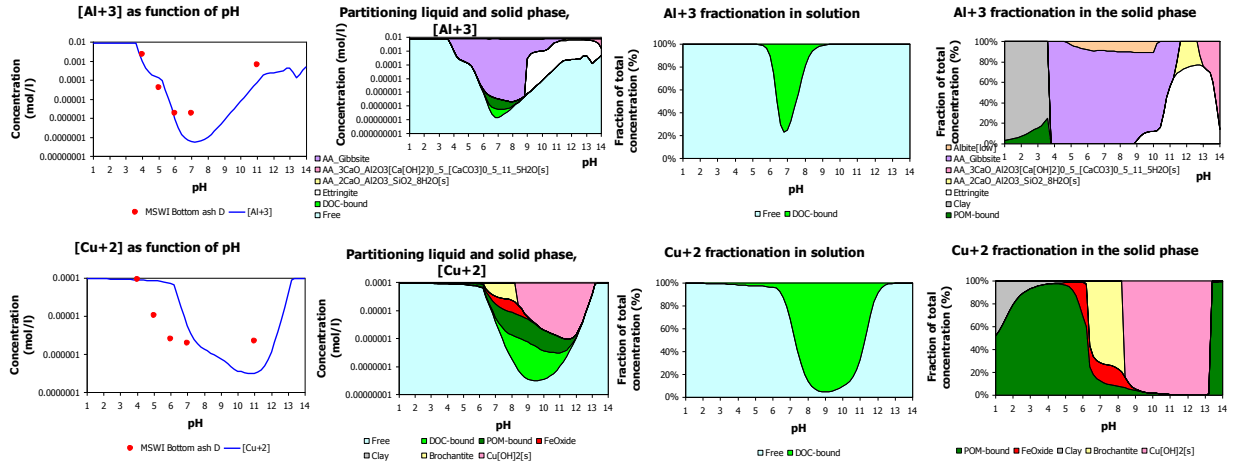

Figure 1. Modeling pH dependence leaching test data for MSWI bottom ash BAM with LeachXS.

Based on a preliminary data evaluation using the availability of salts from the laboratory leaching tests and the observed cumulative release in the lysimeter experiments an indication of the proportion of stagnant versus mobile phase was assessed. In Table II the results for a selection of elements are summarized. From the mobile species (shaded values in Table II), K, SO_4, and Cl, it can be concluded that roughly 70% of the MSWI bottom ash layer is not affected by the leaching process. Only 30 % of the leachable material is available due to preferential flow.

[1] A consistent geochemical modelling approach for the leaching and reactive transport of major and trace elements in MSWI bottom ash. Dijkstra, J.J., Meeussen, J.C.L. and Van der Sloot, H.A. and Comans, R.N. J. *Applied Geochemistry* **23** (6) 1544-1562 June 2008.

Table II Preferential flow information derived from BAM Bottom ash and lysimeter data

Element	Availability mg/kg	Available total mg in lysimeter*	Cumulative release in mg/kg		Note
			mg/kg at L/S2.3	in percent	
Cd	1	870	0.0059	0.59	
Cr	0.73	635	0.086	11.7	
K	828	720360	203	24.5	#
Na	1525	1326750	1080	70.8	?
Pb	16.7	14529	0.043	0.26	
Ni	3.72	3236	0.089	2.38	
SO_4	2446	2128020	655	26.8	#
Cu	60.4	52548	0.086	0.142	
Zn	525	456750	0.42	0.080	
Cl	3500	3045000	1222	34.9	
Ca	24000	20880000	115	0.479	#
Mg	764	664680	20	2.618	
*	Based on a total weight of 870 kg in MSWI bottom ash; soil layer excluded				
#	Corrected for background infiltration				
?	Surprisingly high result in comparison with other highly mobile salts; seems another input of Na has occurred, or Na from soil is non negligible.				

Finally, the information from the pH dependence test (CSF) modeling was used in the 3 layer model to describe release in the GSF lysimeter. The following assumptions were made:

- MSWI bottom ash samples used in GSF lysimeter are the same as the material supplied by BAM
- The missing parameters for modeling Fe-oxide, clay and organic matter were similar to Dutch bottom ashes, which were characterized in more detail
- The soil, for which no data were available is assumed to be a weak sandy soil with assumed parameters for Fe-oxide, Al-oxide, DOC and POM (particulate organic matter) and available metal contents
- Preferential flow is taken from the evaluation in Table III.
- A rainwater composition is assumed as leachant and carbonation is at this stage modeled by CO_3^{2-} in the feed solution.

The following parameters have been used in addition to the CSF to reach a prediction (Table III).

Table III. Input parameters for modeling lysimeter test data

Parameter	Value	Parameter	Value
Flow rate ($l/m^2/s$)	$1.5\ 10^{-5}$		
Waste layer			
pe+pH	13.2	Percent stagnant phase	35
Initial pH	11.2	Transfer parameter – stagnant to mobile phase	15
Porosity	0.35	Column length (cm)	50
Density (kg/dm^3)	1.8	Clay content (kg/kg)	0.01
Fe-oxide kg/kg	0.0002	Solid organic matter (kg/kg)	0.0002
Soil layer			
pe+pH	13	Percent stagnant phase	35
Initial pH	6.2	Transfer parameter – stagnant to mobile phase	4
Porosity	0.35	Column length (cm)	125
Density (kg/dm^3)	1.8	Clay content (kg/kg)	0.01
Fe-oxide kg/kg	0.0002	Solid organic matter (kg/kg)	0.0002
Leachant			
pH	7	K (mol/l)	$1.0\ 10^{-4}$
Cl (mol/l)	4.510^{-4}	Na (mol/l)	$5.0\ 10^{-3}$
Ca (mol/l)	$8.0\ 10^{-5}$	Carbonate (mol/l)	$2.0\ 10^{-3}$
Mg (mol/l)	$1.0\ 10^{-4}$	Sulphate (mol/l)	$6.0\ 10^{-4}$

The transfer factor between stagnant and mobile phase represents a measure of the rate of diffusion from the stagnant zone to the mobile zone. It is expressed as a distance. A value of 1 denotes very direct transfer, while higher factors lead to slower transfer and consequently more tailing. In Figure 2 some selected parameters are given with the modeling results as obtained from full mechanistic modeling of percolation test data (Full data are given in Appendix B).

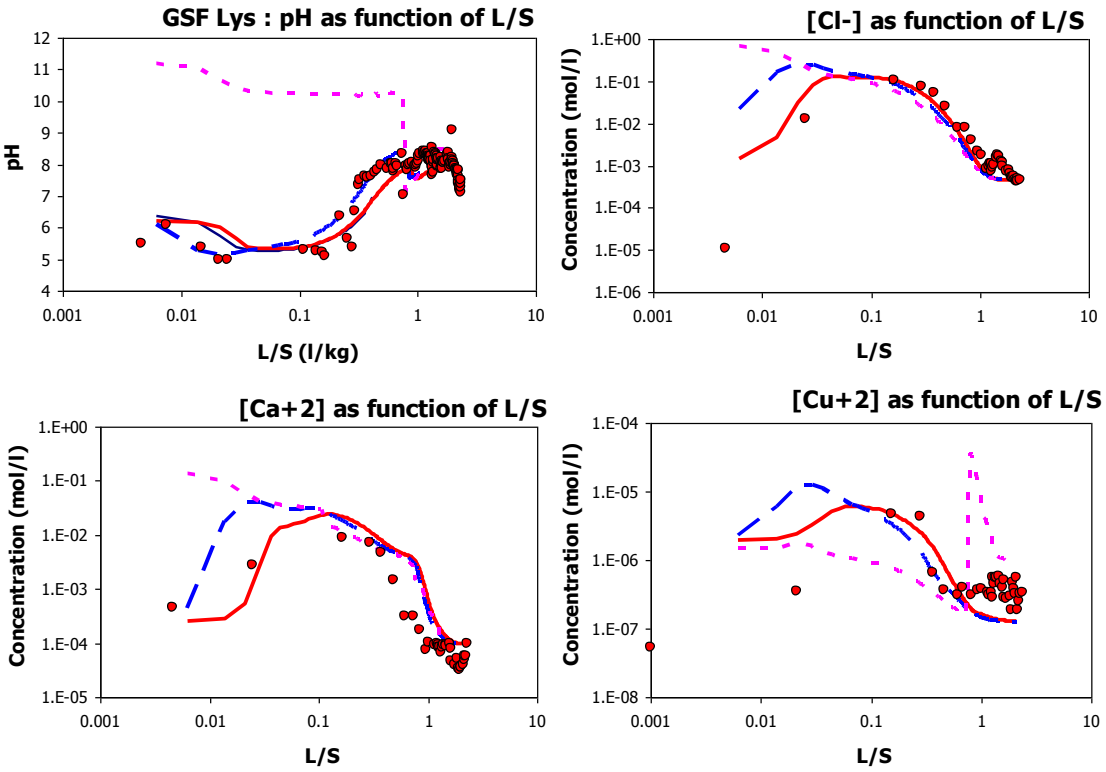

Figure 2. Full mechanistic modeling results (LeachXS-Orchestra) for pH, Cl, Ca and Cu are shown in comparison with data as provided by SIWAP on the GSF lysimeter with MSWI bottom ash. *Legend: red solid line – concentration at bottom of lysimeter (corresponds with the red dots – measurements of leachate); blue broken line – concentrations in soil underneath the bottom ash at a depth of 50 cm into the soil and purple dotted line – concentrations at the bottom ash- soil interface.*

When the scenario is implemented in LeachXS, then the partitioning all along the profile at different exposure times can be provided as well. A more detailed description of particulate and dissolved phases can then be obtained.

The description of DOC release needs to be improved. This affects many elements and is therefore of crucial importance.

Further improvement can be obtained by modeling the percolation experiments on the bottom ash in laboratory experiments and substantial improved can be expected when the sorptive surfaces and missing parameters for bottom ash (e.g. Si, P, Fe, Mo, V) and pH stat information on the underlying soil (no data at all at this point) are better quantified.

APPENDIX A. pH dependence test prediction of MSWI bottom ash (BAM sample SIWAP)

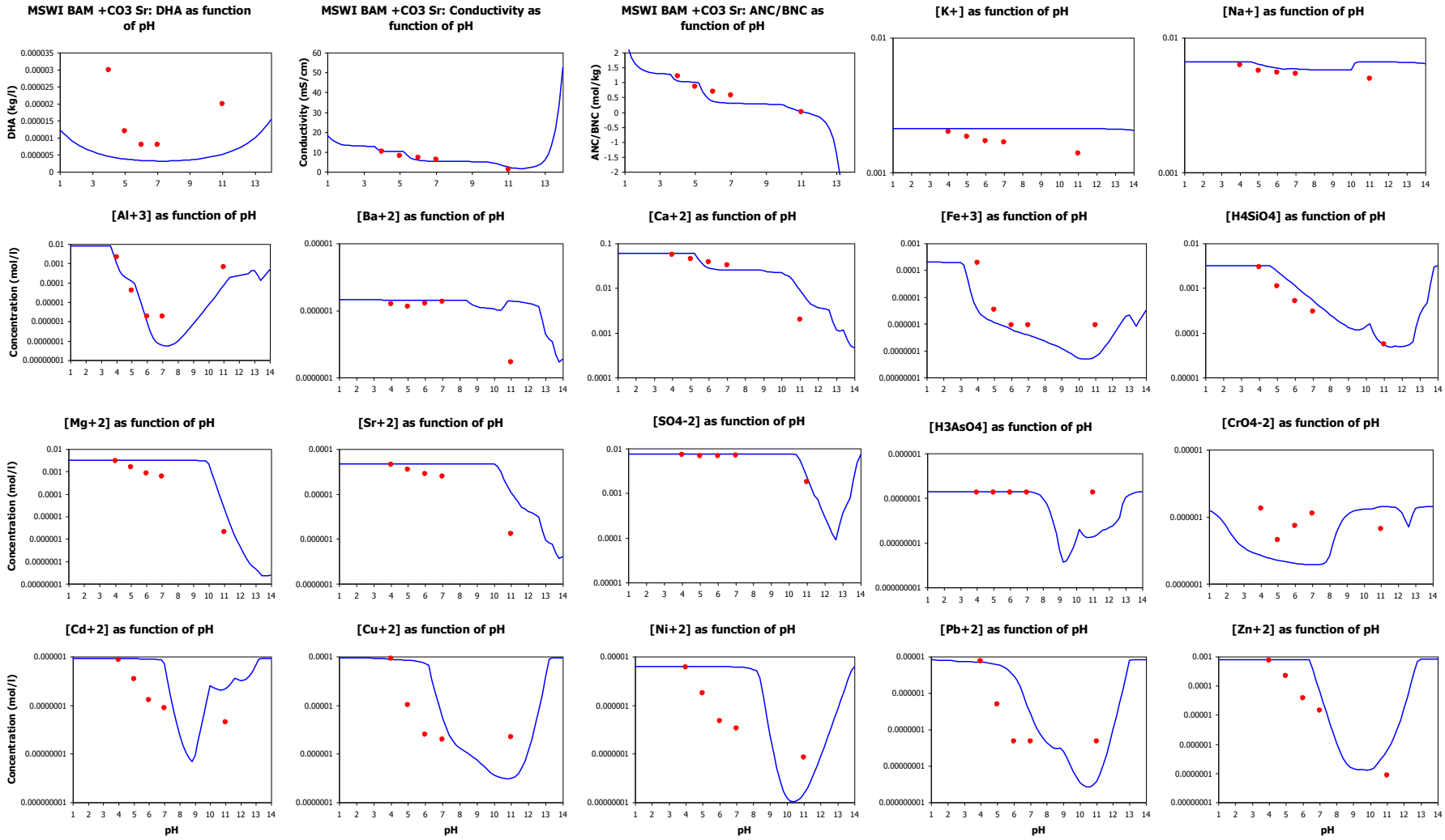

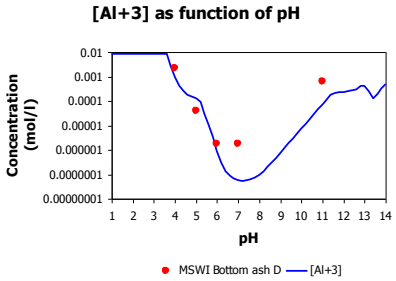
[Al+3] as function of pH
Concentration (mol/l)
pH
MSWI Bottom ash D
[Al+3]

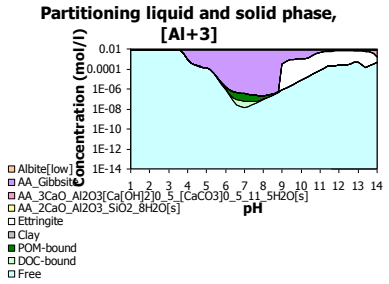
Partitioning liquid and solid phase, [Al+3]
Concentration (mol/l)
pH
Albite[low]
AA_Gibbsite
AA_3CaO_Al2O3[Ca[OH]2]0_5_[CaCO3]0_5_11_5H2O[s]
AA_2CaO_Al2O3_SiO2_8H2O[s]
Ettringite
Clay
POM-bound
DOC-bound
Free

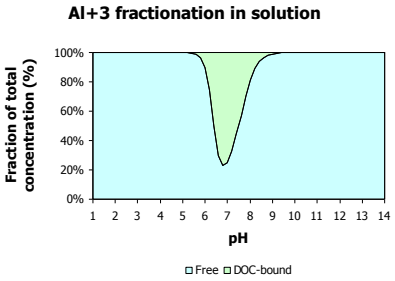
Al+3 fractionation in solution
Fraction of total concentration (%)
pH
Free
DOC-bound

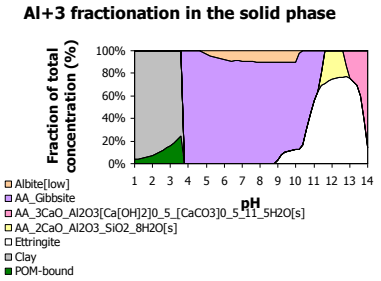
Al+3 fractionation in the solid phase
Fraction of total concentration (%)
pH
Albite[low]
AA_Gibbsite
AA_3CaO_Al2O3[Ca[OH]2]0_5_[CaCO3]0_5_11_5H2O[s]
AA_2CaO_Al2O3_SiO2_8H2O[s]
Ettringite
Clay
POM-bound

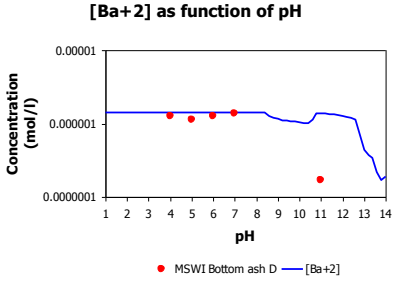
[Ba+2] as function of pH
Concentration (mol/l)
pH
MSWI Bottom ash D
[Ba+2]

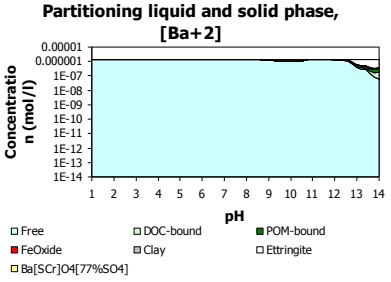
Partitioning liquid and solid phase, [Ba+2]
Concentration (mol/l)
pH
Free
DOC-bound
POM-bound
FeOxide
Clay
Ettringite
Ba[SCr]O4[77%SO4]

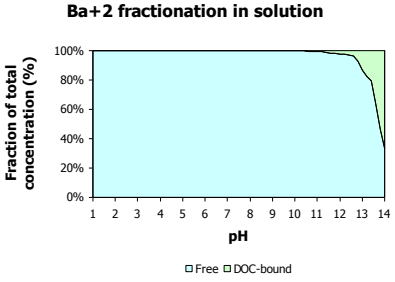
Ba+2 fractionation in solution
Fraction of total concentration (%)
pH
Free
DOC-bound

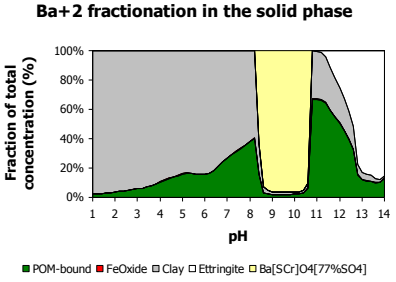
Ba+2 fractionation in the solid phase
Fraction of total concentration (%)
pH
POM-bound
FeOxide
Clay
Ettringite
Ba[SCr]O4[77%SO4]

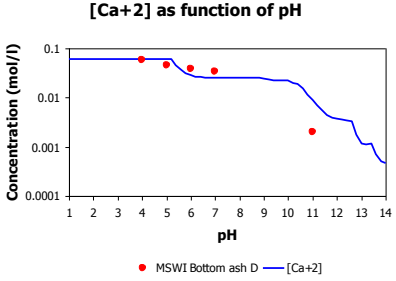
[Ca+2] as function of pH
Concentration (mol/l)
pH
MSWI Bottom ash D
[Ca+2]

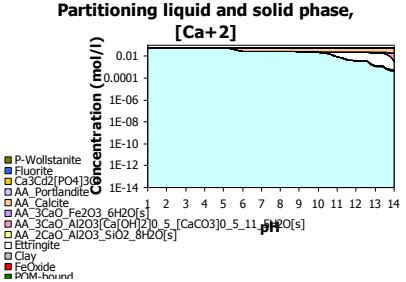
Partitioning liquid and solid phase, [Ca+2]
Concentration (mol/l)
pH
P-Wollstanite
Fluorite
Ca3Cd2[PO4]3Cl
AA_Portlandite
AA_Calcite
AA_3CaO_Fe2O3_6H2O[s]
AA_3CaO_Al2O3[Ca[OH]2]0_5_[CaCO3]0_5_11_5H2O[s]
AA_2CaO_Al2O3_SiO2_8H2O[s]
Ettringite
Clay
FeOxide
POM-bound

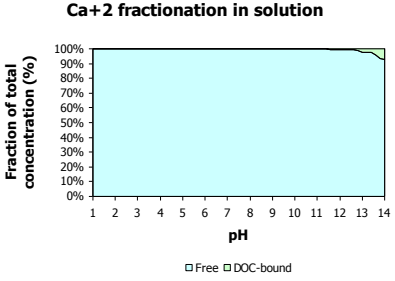
Ca+2 fractionation in solution
Fraction of total concentration (%)
pH
Free
DOC-bound

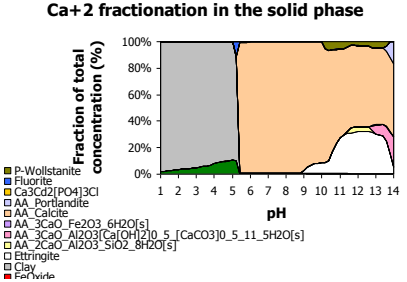
Ca+2 fractionation in the solid phase
Fraction of total concentration (%)
pH
P-Wollstanite
Fluorite
Ca3Cd2[PO4]3Cl
AA_Portlandite
AA_Calcite
AA_3CaO_Fe2O3_6H2O[s]
AA_3CaO_Al2O3[Ca[OH]2]0_5_[CaCO3]0_5_11_5H2O[s]
AA_2CaO_Al2O3_SiO2_8H2O[s]
Ettringite
Clay
FeOxide

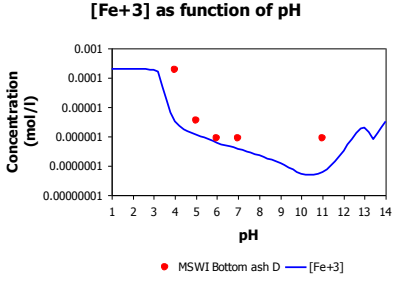
[Fe+3] as function of pH
Concentration (mol/l)
pH
MSWI Bottom ash D
[Fe+3]

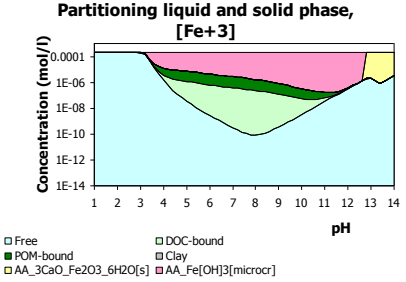
Partitioning liquid and solid phase, [Fe+3]
Concentration (mol/l)
pH
Free
DOC-bound
POM-bound
Clay
AA_3CaO_Fe2O3_6H2O[s]
AA_Fe[OH]3[microcr]

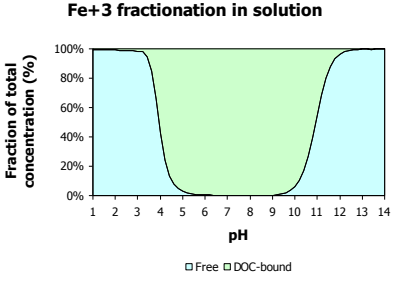
Fe+3 fractionation in solution
Fraction of total concentration (%)
pH
Free
DOC-bound

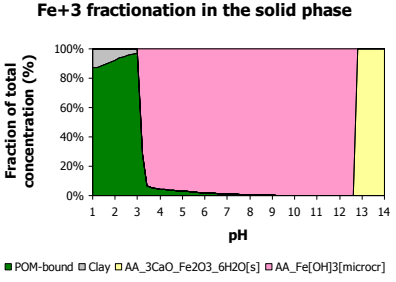
Fe+3 fractionation in the solid phase
Fraction of total concentration (%)
pH
POM-bound
Clay
AA_3CaO_Fe2O3_6H2O[s]
AA_Fe[OH]3[microcr]

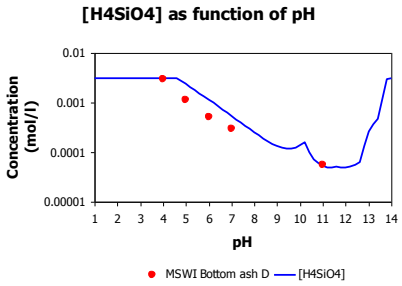
[H4SiO4] as function of pH
Concentration (mol/l)
pH
MSWI Bottom ash D
[H4SiO4]

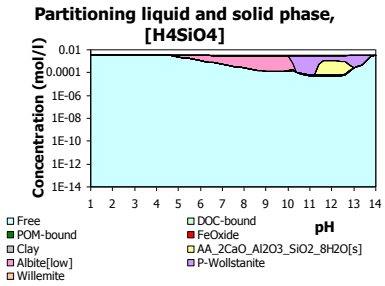
Partitioning liquid and solid phase, [H4SiO4]
Concentration (mol/l)
pH
Free
DOC-bound
POM-bound
FeOxide
Clay
AA_2CaO_Al2O3_SiO2_8H2O[s]
Albite[low]
P-Wollstanite
Willemite

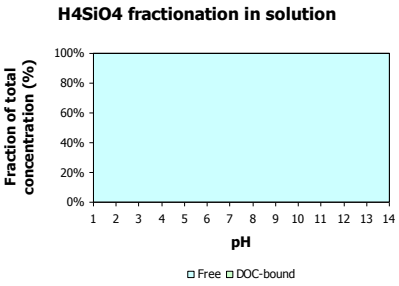
H4SiO4 fractionation in solution
Fraction of total concentration (%)
pH
Free
DOC-bound

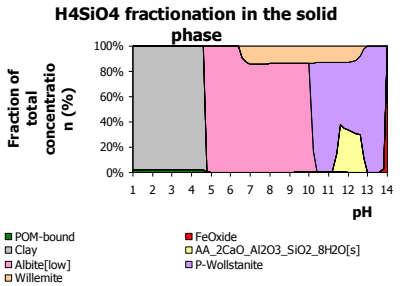
H4SiO4 fractionation in the solid phase
Fraction of total concentratio n (%)
pH
POM-bound
FeOxide
Clay
AA_2CaO_Al2O3_SiO2_8H2O[s]
Albite[low]
P-Wollstanite
Willemite

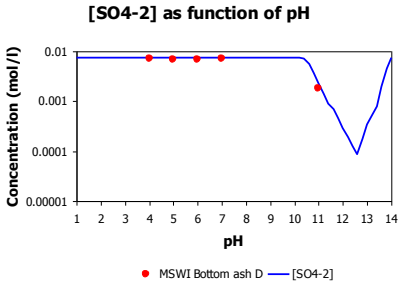
[SO4-2] as function of pH
Concentration (mol/l)
pH
MSWI Bottom ash D
[SO4-2]

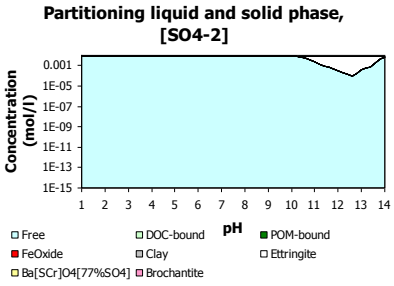
Partitioning liquid and solid phase, [SO4-2]
Concentration (mol/l)
pH
Free
DOC-bound
POM-bound
FeOxide
Clay
Ettringite
Ba[SCr]O4[77%SO4]
Brochantite

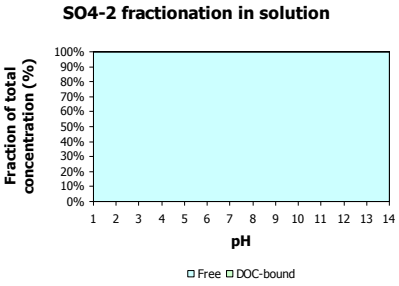
SO4-2 fractionation in solution
Fraction of total concentration (%)
pH
Free
DOC-bound

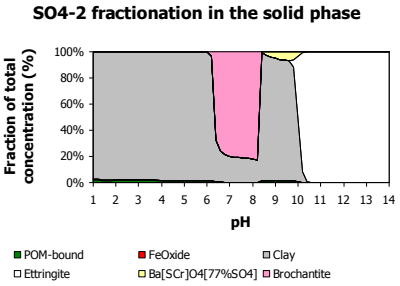
SO4-2 fractionation in the solid phase
Fraction of total concentration (%)
pH
POM-bound
FeOxide
Clay
Ettringite
Ba[SCr]O4[77%SO4]
Brochantite

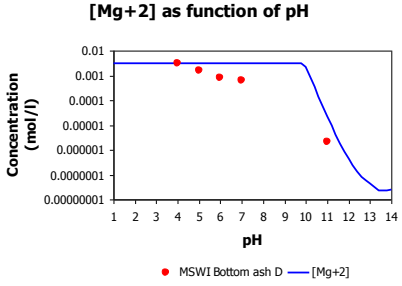
[Mg+2] as function of pH
Concentration (mol/l)
pH
MSWI Bottom ash D
[Mg+2]

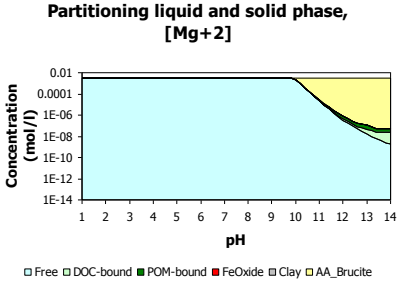
Partitioning liquid and solid phase, [Mg+2]
Concentration (mol/l)
pH
Free
DOC-bound
POM-bound
FeOxide
Clay
AA_Brucite

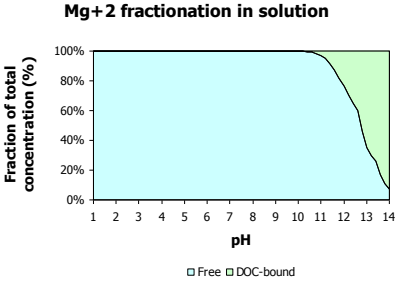
Mg+2 fractionation in solution
Fraction of total concentration (%)
pH
Free
DOC-bound

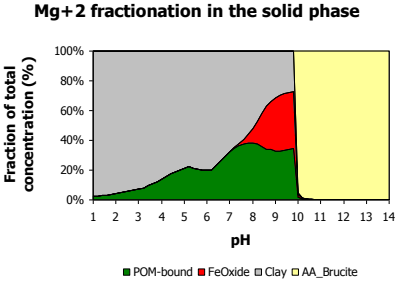
Mg+2 fractionation in the solid phase
Fraction of total concentration (%)
pH
POM-bound
FeOxide
Clay
AA_Brucite

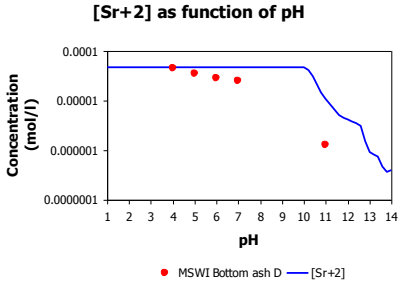
[Sr+2] as function of pH
Concentration (mol/l)
pH
MSWI Bottom ash D
[Sr+2]

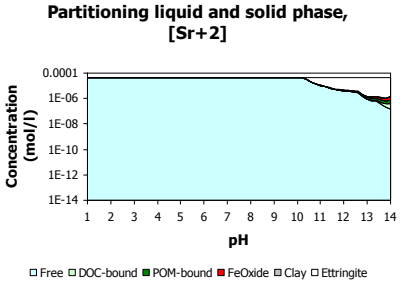
Partitioning liquid and solid phase, [Sr+2]
Concentration (mol/l)
pH
Free
DOC-bound
POM-bound
FeOxide
Clay
Ettringite

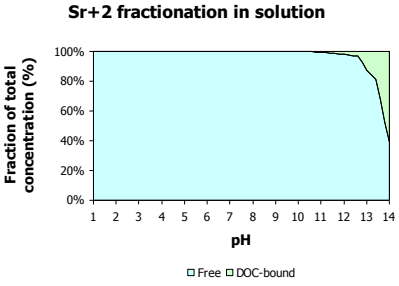
Sr+2 fractionation in solution
Fraction of total concentration (%)
pH
Free
DOC-bound

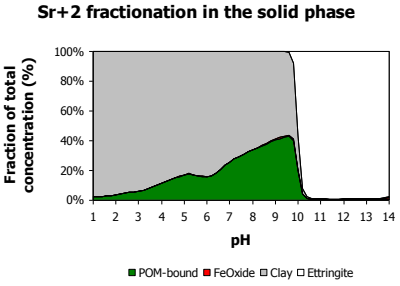
Sr+2 fractionation in the solid phase
Fraction of total concentration (%)
pH
POM-bound
FeOxide
Clay
Ettringite

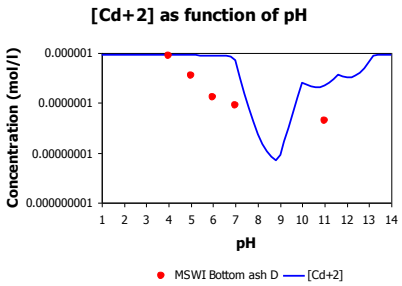
[Cd+2] as function of pH
Concentration (mol/l)
0.000001
0.0000001
0.00000001
0.000000001
1 2 3 4 5 6 7 8 9 10 11 12 13 14
pH
MSWI Bottom ash D
[Cd+2]

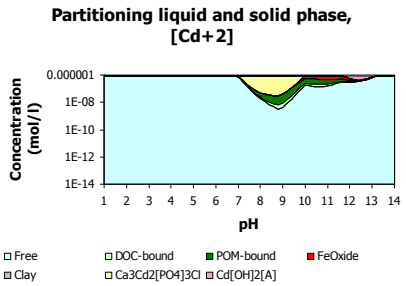
Partitioning liquid and solid phase, [Cd+2]
Concentration (mol/l)
0.000001
1E-08
1E-10
1E-12
1E-14
1 2 3 4 5 6 7 8 9 10 11 12 13 14
pH
Free
DOC-bound
POM-bound
FeOxide
Clay
Ca3Cd2[PO4]3Cl
Cd[OH]2[A]

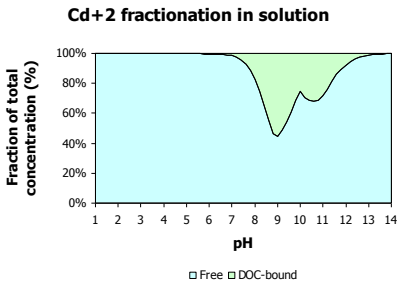
Cd+2 fractionation in solution
Fraction of total concentration (%)
100%
80%
60%
40%
20%
0%
1 2 3 4 5 6 7 8 9 10 11 12 13 14
pH
Free
DOC-bound

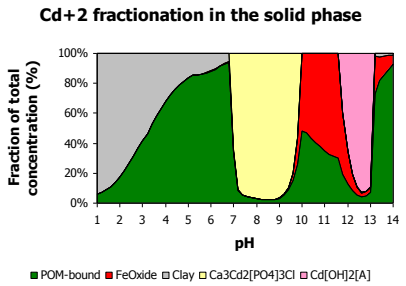
Cd+2 fractionation in the solid phase
Fraction of total concentration (%)
100%
80%
60%
40%
20%
0%
1 2 3 4 5 6 7 8 9 10 11 12 13 14
pH
POM-bound
FeOxide
Clay
Ca3Cd2[PO4]3Cl
Cd[OH]2[A]

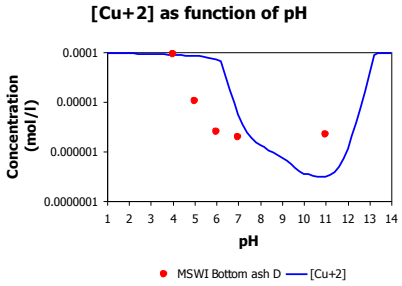
[Cu+2] as function of pH
Concentration (mol/l)
0.0001
0.00001
0.000001
0.0000001
1 2 3 4 5 6 7 8 9 10 11 12 13 14
pH
MSWI Bottom ash D
[Cu+2]

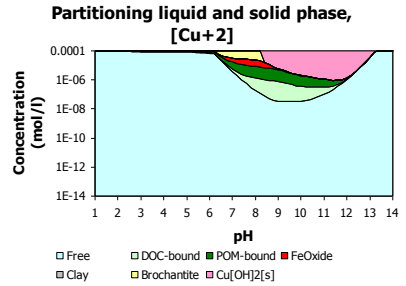
Partitioning liquid and solid phase, [Cu+2]
Concentration (mol/l)
0.0001
1E-06
1E-08
1E-10
1E-12
1E-14
1 2 3 4 5 6 7 8 9 10 11 12 13 14
pH
Free
DOC-bound
POM-bound
FeOxide
Clay
Brochantite
Cu[OH]2[s]

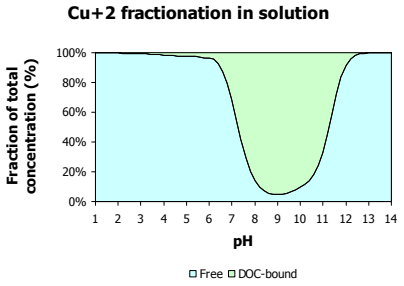
Cu+2 fractionation in solution
Fraction of total concentration (%)
100%
80%
60%
40%
20%
0%
1 2 3 4 5 6 7 8 9 10 11 12 13 14
pH
Free
DOC-bound

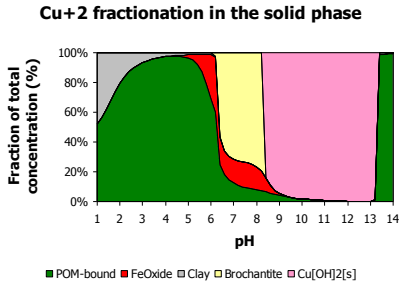
Cu+2 fractionation in the solid phase
Fraction of total concentration (%)
100%
80%
60%
40%
20%
0%
1 2 3 4 5 6 7 8 9 10 11 12 13 14
pH
POM-bound
FeOxide
Clay
Brochantite
Cu[OH]2[s]

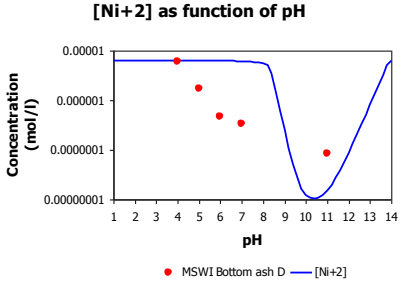
[Ni+2] as function of pH
Concentration (mol/l)
0.00001
0.000001
0.0000001
0.00000001
1 2 3 4 5 6 7 8 9 10 11 12 13 14
pH
MSWI Bottom ash D
[Ni+2]

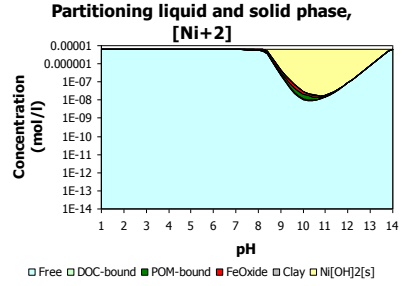
Partitioning liquid and solid phase, [Ni+2]
Concentration (mol/l)
0.00001
0.000001
1E-07
1E-08
1E-09
1E-10
1E-11
1E-12
1E-13
1E-14
1 2 3 4 5 6 7 8 9 10 11 12 13 14
pH
Free
DOC-bound
POM-bound
FeOxide
Clay
Ni[OH]2[s]

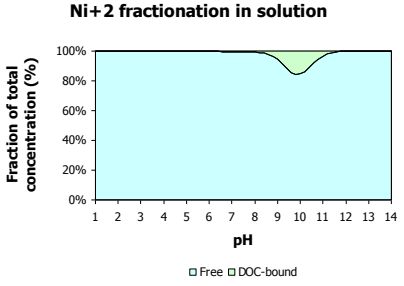
Ni+2 fractionation in solution
Fraction of total concentration (%)
100%
80%
60%
40%
20%
0%
1 2 3 4 5 6 7 8 9 10 11 12 13 14
pH
Free
DOC-bound

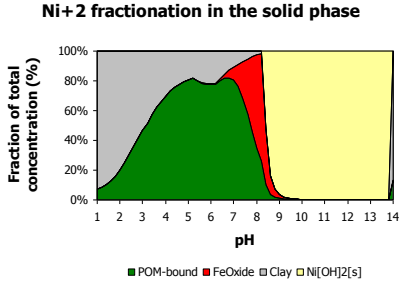
Ni+2 fractionation in the solid phase
Fraction of total concentration (%)
100%
80%
60%
40%
20%
0%
1 2 3 4 5 6 7 8 9 10 11 12 13 14
pH
POM-bound
FeOxide
Clay
Ni[OH]2[s]

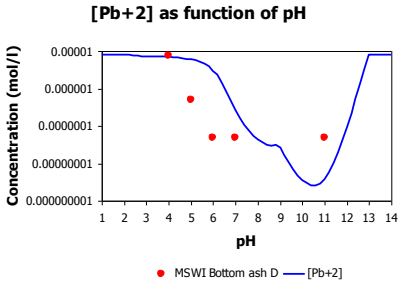
[Pb+2] as function of pH
Concentration (mol/l)
0.00001
0.000001
0.0000001
0.00000001
0.000000001
1 2 3 4 5 6 7 8 9 10 11 12 13 14
pH
MSWI Bottom ash D
[Pb+2]

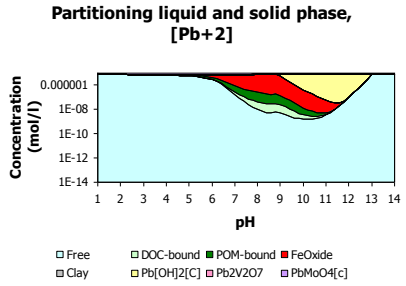
Partitioning liquid and solid phase, [Pb+2]
Concentration (mol/l)
0.000001
1E-08
1E-10
1E-12
1E-14
1 2 3 4 5 6 7 8 9 10 11 12 13 14
pH
Free
DOC-bound
POM-bound
FeOxide
Clay
Pb[OH]2[C]
Pb2V2O7
PbMoO4[c]

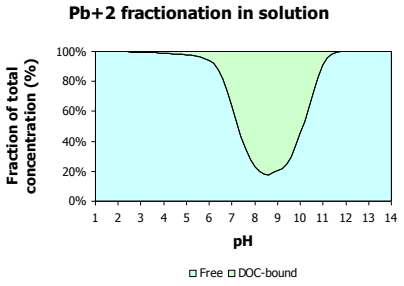
Pb+2 fractionation in solution
Fraction of total concentration (%)
100%
80%
60%
40%
20%
0%
1 2 3 4 5 6 7 8 9 10 11 12 13 14
pH
Free
DOC-bound

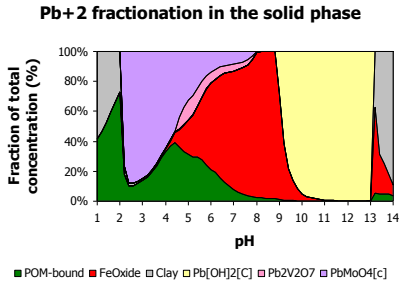
Pb+2 fractionation in the solid phase
Fraction of total concentration (%)
100%
80%
60%
40%
20%
0%
1 2 3 4 5 6 7 8 9 10 11 12 13 14
pH
POM-bound
FeOxide
Clay
Pb[OH]2[C]
Pb2V2O7
PbMoO4[c]

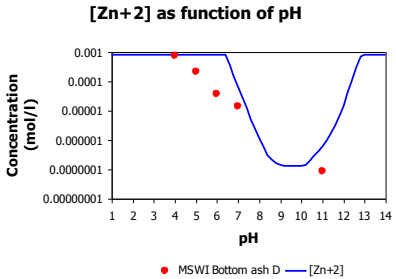
[Zn+2] as function of pH
Concentration (mol/l)
pH
MSWI Bottom ash D
[Zn+2]

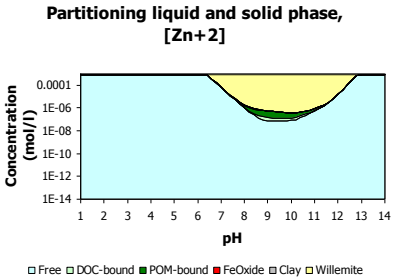
Partitioning liquid and solid phase, [Zn+2]
Concentration (mol/l)
pH
Free
DOC-bound
POM-bound
FeOxide
Clay
Willemite

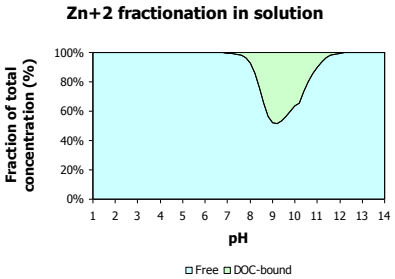
Zn+2 fractionation in solution
Fraction of total concentration (%)
pH
Free
DOC-bound

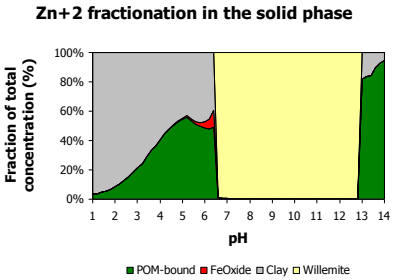
Zn+2 fractionation in the solid phase
Fraction of total concentration (%)
pH
POM-bound
FeOxide
Clay
Willemite

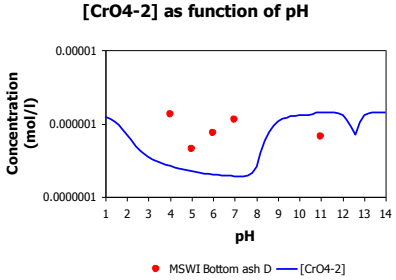
[CrO4-2] as function of pH
Concentration (mol/l)
pH
MSWI Bottom ash D
[CrO4-2]

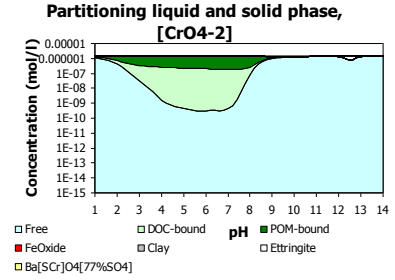
Partitioning liquid and solid phase, [CrO4-2]
Concentration (mol/l)
pH
Free
DOC-bound
POM-bound
FeOxide
Clay
Ettringite
Ba[SCr]O4[77%SO4]

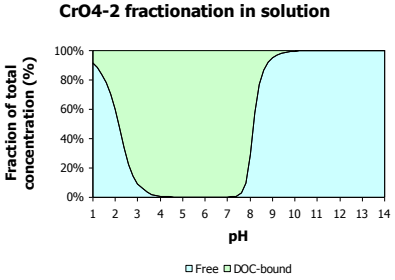
CrO4-2 fractionation in solution
Fraction of total concentration (%)
pH
Free
DOC-bound

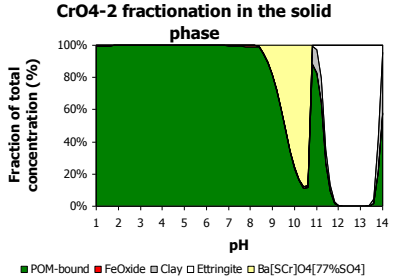
CrO4-2 fractionation in the solid phase
Fraction of total concentration (%)
pH
POM-bound
FeOxide
Clay
Ettringite
Ba[SCr]O4[77%SO4]

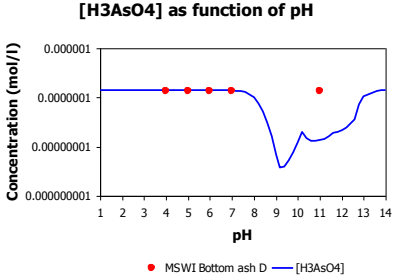
[H3AsO4] as function of pH
Concentration (mol/l)
pH
MSWI Bottom ash D
[H3AsO4]

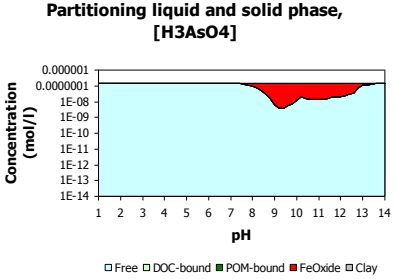
Partitioning liquid and solid phase, [H3AsO4]
Concentration (mol/l)
pH
Free
DOC-bound
POM-bound
FeOxide
Clay

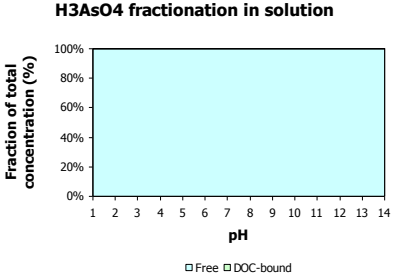
H3AsO4 fractionation in solution
Fraction of total concentration (%)
pH
Free
DOC-bound

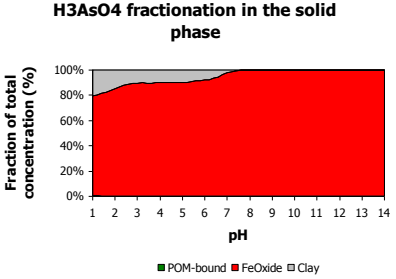
H3AsO4 fractionation in the solid phase
Fraction of total concentration (%)
pH
POM-bound
FeOxide
Clay

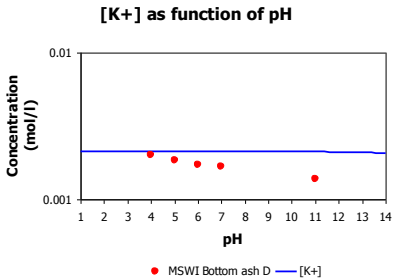
[K+] as function of pH
Concentration (mol/l)
pH
MSWI Bottom ash D
[K+]

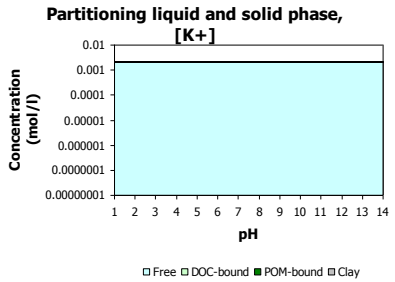
Partitioning liquid and solid phase, [K+]
Concentration (mol/l)
pH
Free
DOC-bound
POM-bound
Clay

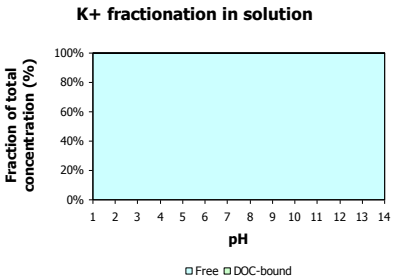
K+ fractionation in solution
Fraction of total concentration (%)
pH
Free
DOC-bound

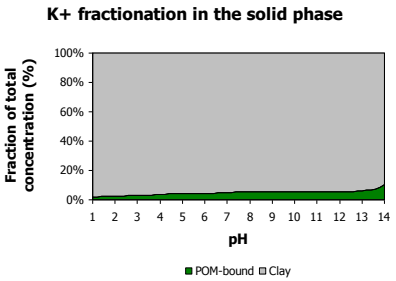
K+ fractionation in the solid phase
Fraction of total concentration (%)
pH
POM-bound
Clay

APPENDIX B. Results from a 2 layer (bottom ash – soil) model with dual porosity.

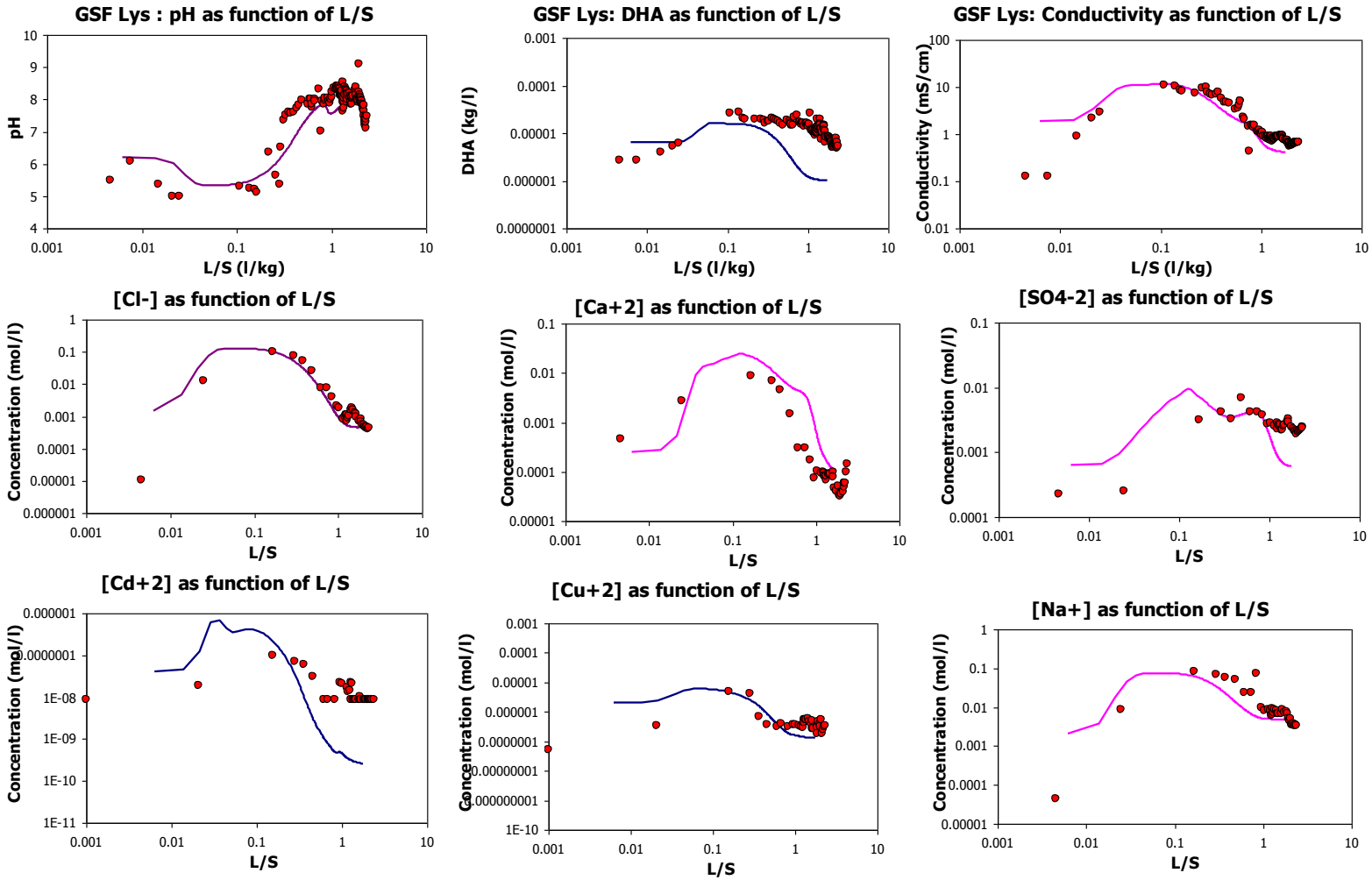

Parameters pH, DOC, EC, Cl, Ca, SO_4, Cd, Cu and Na on a logarithmic x-axis

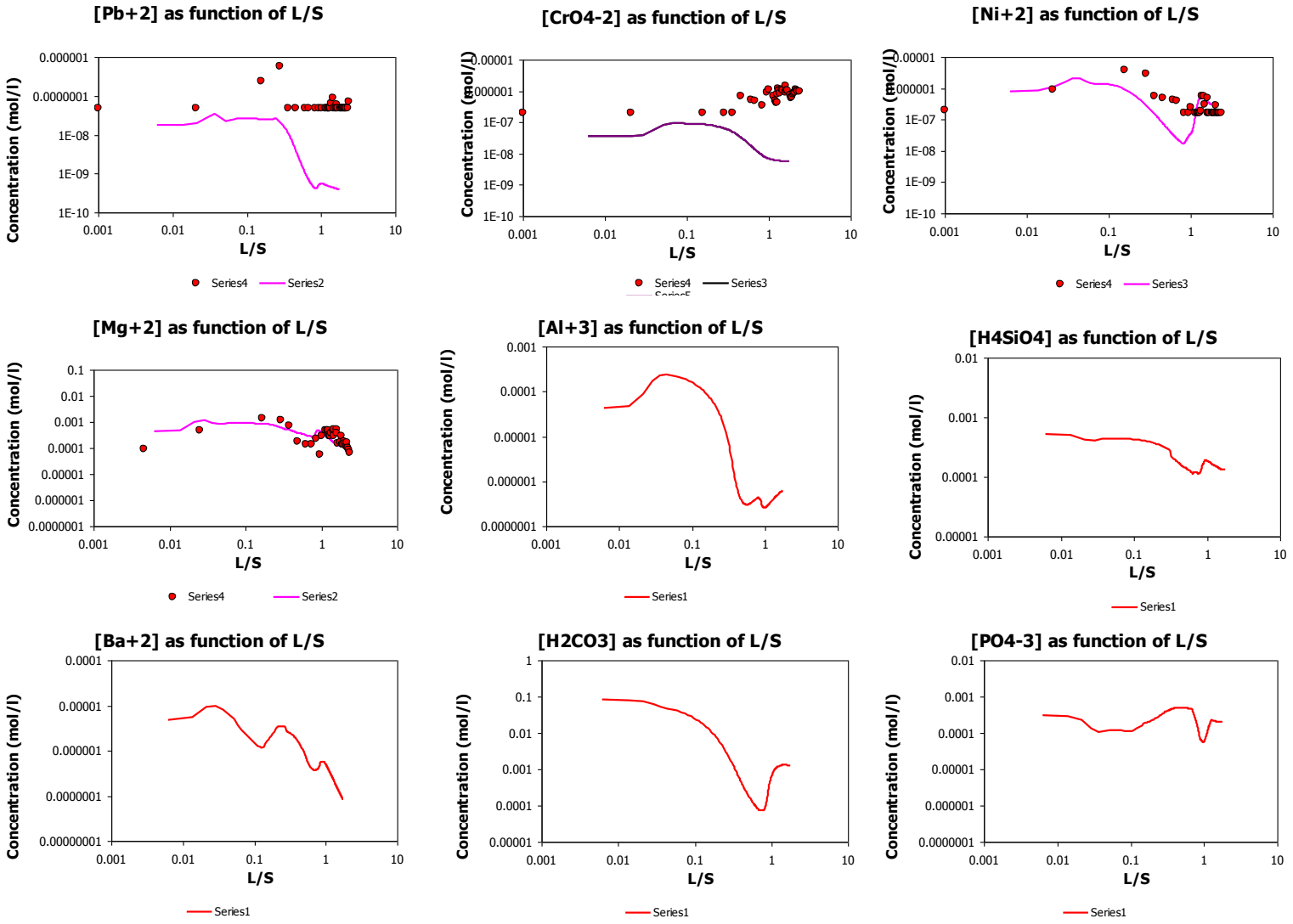

Parameters Pb, Cr, Ni, Mg, Al, Si, Ba, carbonate and PO_4 on a logarithmic x-axis (no field data for 5 last parameters)

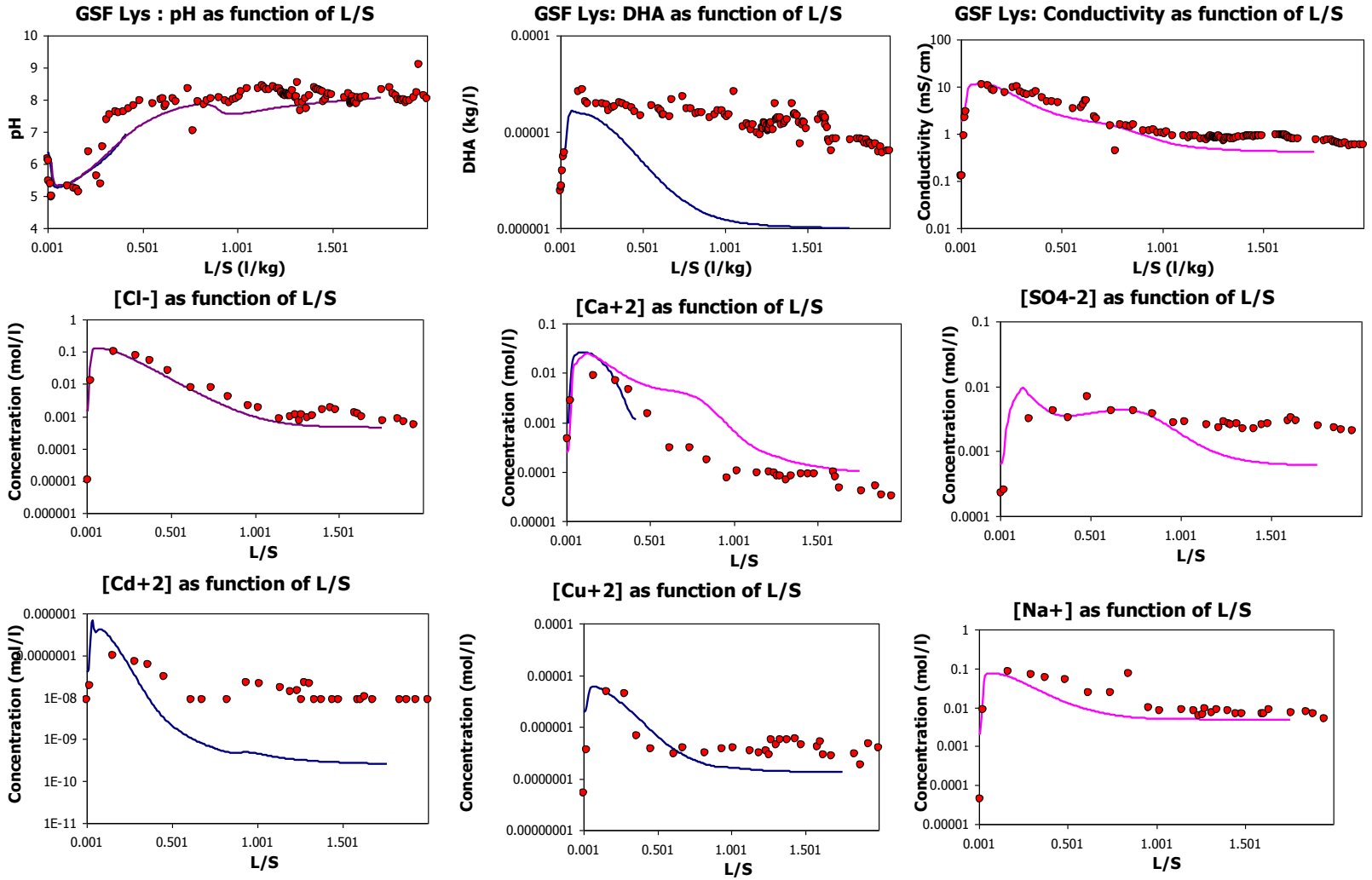

Parameters pH, DOC, EC, Cl, Ca, SO_4, Cd, Cu and Na on a linear x-axis